

CHAPTER IITHE EXPERIMENTAL SET UP.2.1. Introduction:-

In this dissertation experimental observation and theoretical interpretation of some of the physical processes occurring in the glow and arc discharge plasma both in the absence and in the presence of either transverse or longitudinal magnetic field have been undertaken. In this investigation the plasma parameters of the glow (excited by ac and rf sources) and arc discharges have been estimated utilizing different techniques, electrical and spectroscopic under immersive and non-immersive probe schemes.

For the study of plasma behaviour we utilise the positive column of the discharges excited by ac and rf discharges, low pressure mercury arc and metal arcs in air with three different types of electrodes (i) silver-silver, (ii) copper-copper and (iii) iron-iron.

To study the effect of magnetic field a low pressure plasma with a low input energy has been taken, because plasma transport properties will be more influenced by the magnetic field as in low pressure discharge the mean free times of the plasma species are

large. It is also worthwhile to note that in case of low pressure arc, before any set of observations is made, a steady state of the discharge has initially been achieved, there after the plasma parameters under interest have been investigated.

## 2.2. Discharge tubes&arc tubes:

Discharge tubes used in experimental measurements were constructed of pyrex glass. For glow discharge measurements the tubes were fitted with steel electrodes to minimize the sputtering yield. The external voltage has been applied to two circular parallel plate electrodes for breakdown. All arc tubes in which experiments have been carried out are also made of pyrex glass. The arcs have been produced between two mercury pool electrodes (fitted with two tungsten wires for external electrical connections) by a 250 volt dc source from a dc generator. Fig. 2.1 shows the design and construction of all arc tubes used in the laboratory. They are fitted to simple traps so that the mercury vapour going out of the discharge tube could condense smoothly and could return to the tube. Otherwise, it was observed that mercury would condense in the connecting rubber tubes and a mercury plug would be formed in

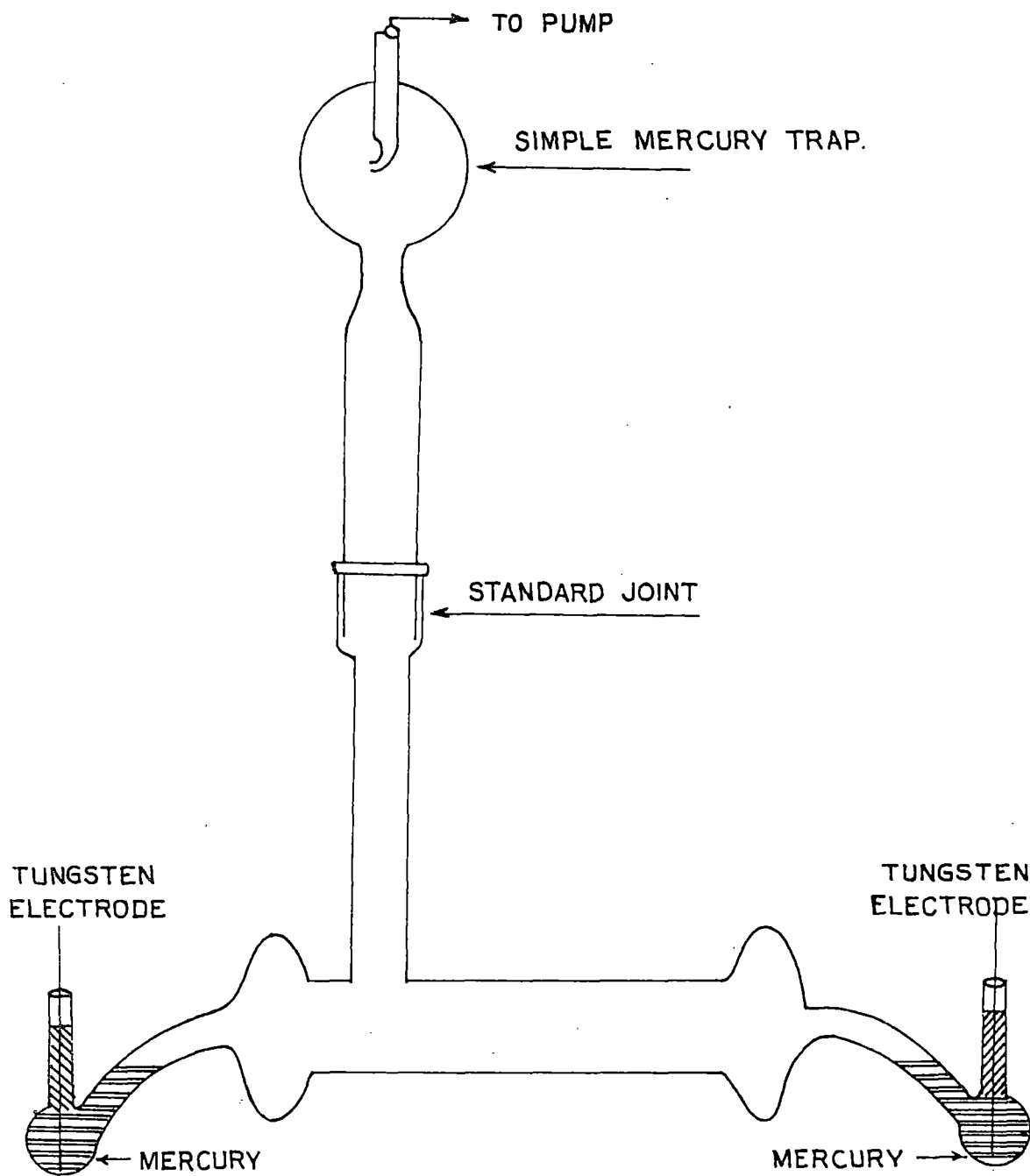


FIG. 2.1. DIAGRAM OF A MERCURY ARC TUBE .

the passage and thereby would disturb the vacuum system. The whole arc system is cooled down by air coolers and two mercury pool electrodes by circulation of water.

### 2.3. Cleaning and processing of arc tube:

For the preparation of mercury arc the arc tube is thoroughly washed and cleaned with dilute chromic acid and then with NaOH solution. The tube is then washed several times with distilled water and then with dehydrated benzene. The tubes are then heat baked in an electrical oven. Triple distilled mercury is then poured into the tube to the desired level. The tube is then connected to a double stage rotary vacuum pump and a vacuum of the order of  $10^{-2}$  torr is achieved.

### 2.4. Preparation of gases for glow discharge:

For measurements where air acts as a buffer, air has been passed through dilute solution of caustic potash to remove traces of  $\text{CO}_2$  and is then washed with water by passing through series of wash bottle containing cold water to remove traces of caustic potash, dust particles and organic matters. It has been dried by passing through a tower of fused  $\text{CaCl}_2$  and finally through  $\text{P}_2\text{O}_5$ . Then air is introduced to a discharge tube and controlled through a needle valve. Hydrogen gas is

prepared from electrolysis of a solution of pure barium hydroxide in between platinum electrodes in a U-tube. For hydrogen, the gas evolved from the cathode was passed through a hard glass tube containing copper spiral heated electrically. The gas is next passed through the same arrangement described above. After purification has been done in stated manners the gases are stored in a round bottomed glass flask which is connected to the discharge tube.

For usual discharge tubes, after several days of run for outgassing and observation purposes, the glass wall would become coated by impurity materials due to sputtering of the cathode. For that reason steel electrodes are used.

## 2.5. Measurements of pressure:

By utilizing McLeod gauge the pressure of the gas in the discharge tube is measured. As shown in fig. 2.2, a parallel line is used for the measurement of pressure in the discharge tube. At the junction between these two vacuum lines the pressure is the same and if the conductance of the two lines are identical, the pressure in the discharge tube would be equal to that at the McLeod gauge. Dushman and Lafferty (1962) have discussed that effective pumping speed,  $S_{eff}$  is given

$$\frac{1}{S_{eff}} = \frac{1}{S} + \frac{1}{C} \quad \dots(2.1)$$

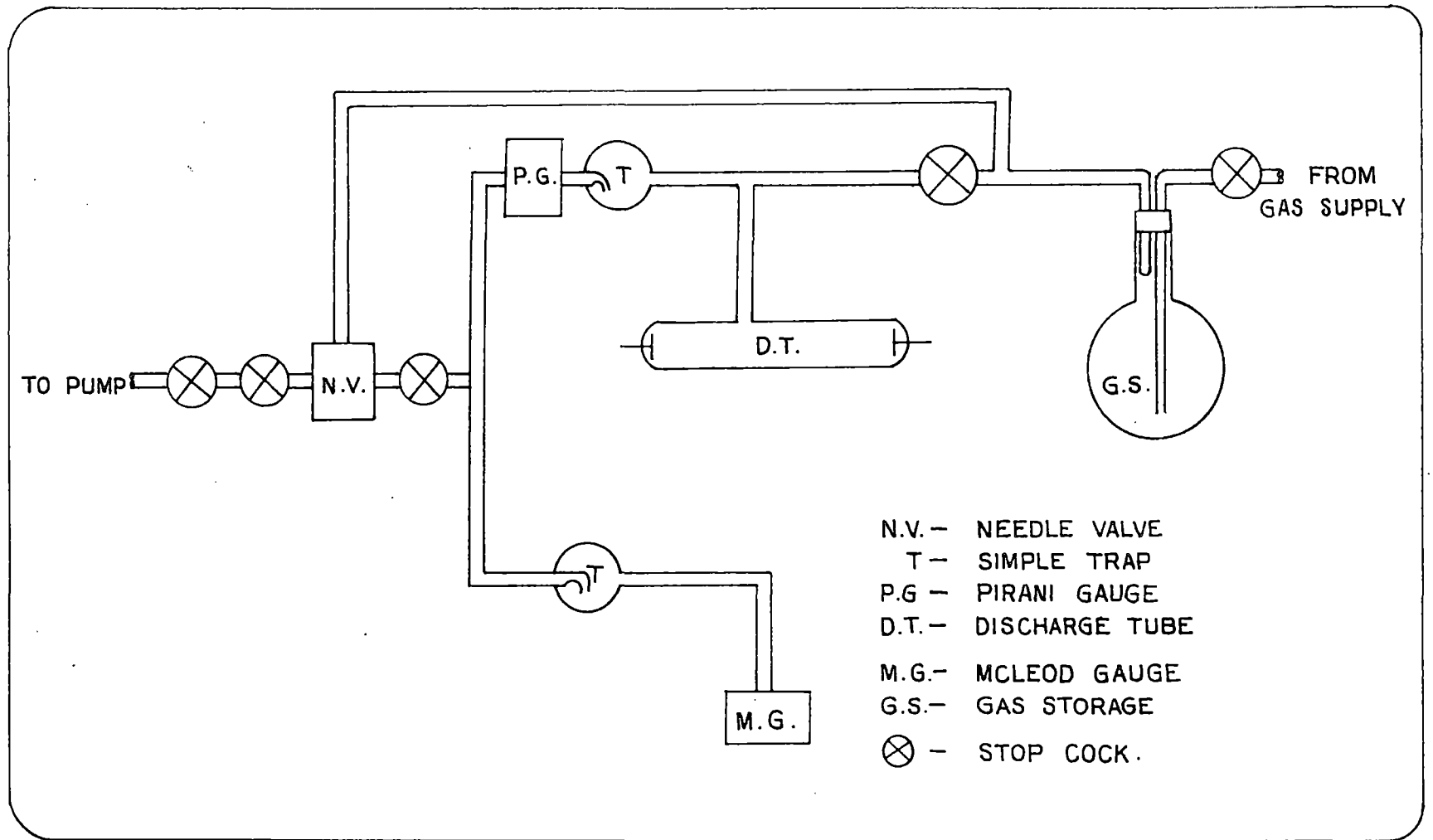


FIG. 2-2. DIAGRAM OF A GLOW DISCHARGE TUBE.

where  $S$  is the speed of the pump (50 litres/min) and  $C$  is the total conductance of the line. For viscous flow, conductance of a line is given by

$$C = 2.84 \frac{a^4}{l} P_2 \text{ litre/ Sec. } \dots(2.2)$$

where  $a$  and  $l$  are the radius and length of the tubes and  $P_2$  is the upstream pressure. The parallel lines as shown in fig. 2.2 are identical as far as possible. The lines are made of rubber and polythene pressure tubes. The needle valve is placed in between the junction of identical lines and the pump for the same reason. A pirani gauge is used in the discharge tube line and through it the pressure of air can be compared. In glow discharge tubes, the order of pressures ranges from 1 to  $10^{-1}$  torr.

In case of arc, a pirani gauge has been used in the arc tube line and through it the pressure of background dry air (buffer gas) has been measured. A needle valve has been placed in the arc tube line to allow a microleak for adjustment of air pressure inside the system.

The pressure of mercury vapour has been measured from standard tables (Hodgman, 1956) after calculating inside wall temperature  $T_w$  of the tube which is equal to the outside wall temperature increased by the

temperature drop over the tube wall resulting from the impact of energy which is dissipated in the tube and carried away via the tube wall (Verweij, 1960). The outside wall temperature has been measured by a mercury in glass thermometer when the arc exists in a steady state condition. In the experiments the arcs have been cooled down by air coolers. Therefore, a steady outerwall temperature corresponds to a steady condition of the arc under investigation. After Verweij, (1960) the temperature drop has been estimated by considering the total energy dissipated  $W = E i$  per cm. along the tube length. Here  $E$  is the magnitude of electric field measured by noting the voltage drop across the arc minus standard cathode fall of 10 volts as measured by Lamar and Compton (1931), then divided by the entire arc length and  $i$  is the arc current. In fact, the amount of energy which escapes as radiation through the tube wall is comparatively small and the ultraviolet resonance radiation is absorbed within a very small penetrating depth in pyrex glass wall of the arc tube. Therefore the dissipated energy flux is carried away mainly by thermal conduction through the surface area of 1 cm. of the arc tube length, hence through  $2 \pi R$  sq.cm. ( $R$  is the inner tube radius).

The temperature drop  $\Delta T_W$  is given by

$$W = 2 \pi R K \frac{\Delta T_W}{d} \quad \dots(2.3)$$

where  $K$  is the thermal conductivity of the glass ( $K_{\text{pyrex}} = 11 \times 10^{-3}$  joule/cm/sec/ $^{\circ}\text{C}$ ) and  $d$  is the thickness of glass wall. For a typical operation of arc at a current of 2.5 A,  $\Delta T_w$  has been estimated to be  $7-8^{\circ}\text{C}$ . A plot of saturated vapour pressure of mercury ( $P_{\text{Hg}}$ ) with  $T_w$  has been shown in fig.2.3. As number density of ground state mercury atoms  $N_g$  is explicitly related with  $P_{\text{Hg}}$  by the relation

$$N_g = 3.3 \times 10^{16} \frac{P_{\text{Hg}}}{T_w} \dots(2.4)$$

$N_g$  has also been plotted against  $T_w$  in the fig.2.3.

## 2.6. Magnets and power supplies:

Magnetic field has been produced by an electromagnet. Depending upon the length and diameter of arc tube/glow tube, gap between the pole pieces of electromagnets has been adjusted. For accuracy in measurement, the pole-pieces have been so chosen that the magnetic field was uniform and without having any radial magnetic field component. For investigation in longitudinal magnetic fields, the total arc tube has been placed in between the pole pieces as shown in fig. 2.4, when a transverse magnetic field is utilized only certain portion of the positive column of

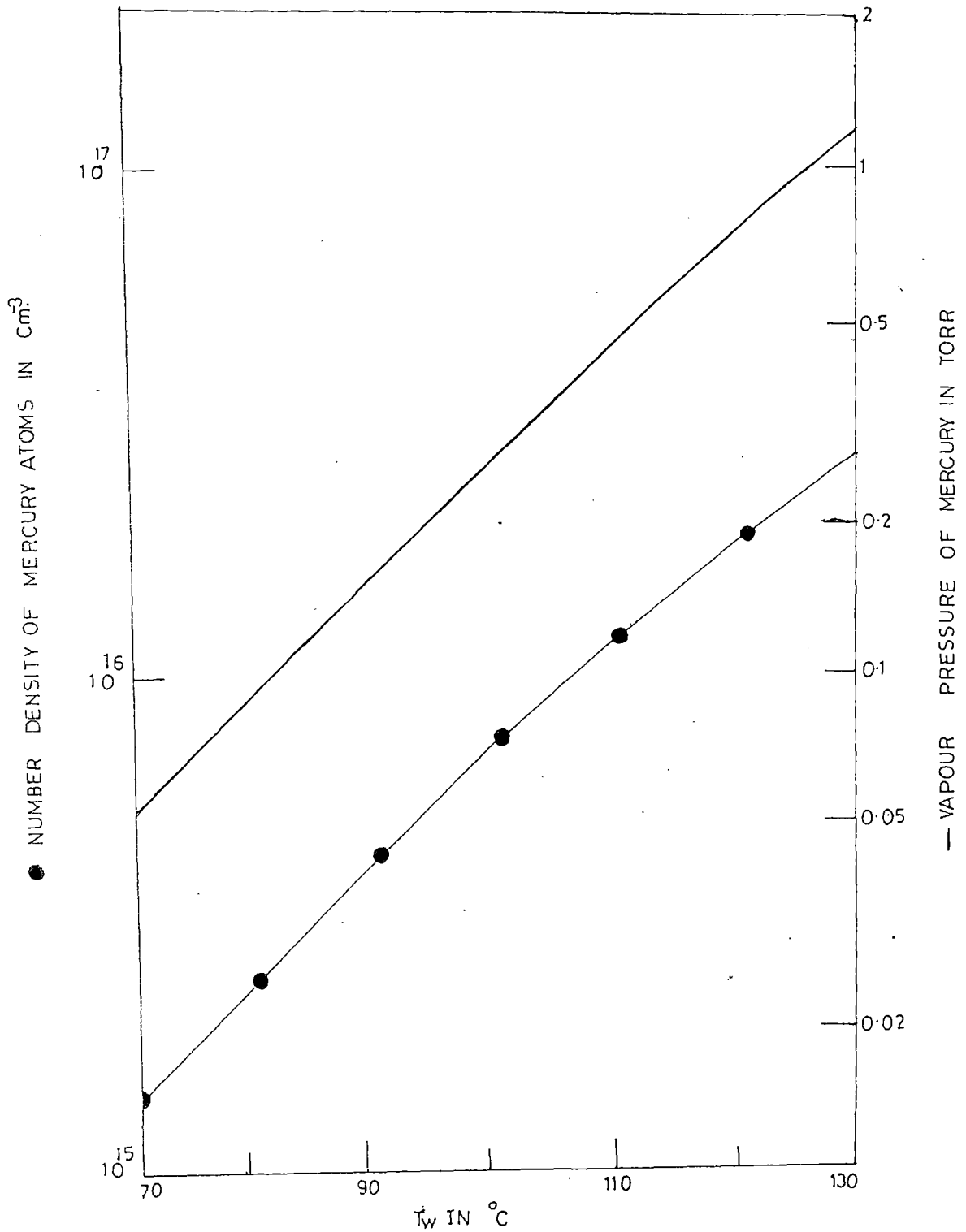


Fig. 2.3. Variation of vapour pressure and number density of mercury atoms with temperature of outer wall ( $T_w$ ) of discharge tube.

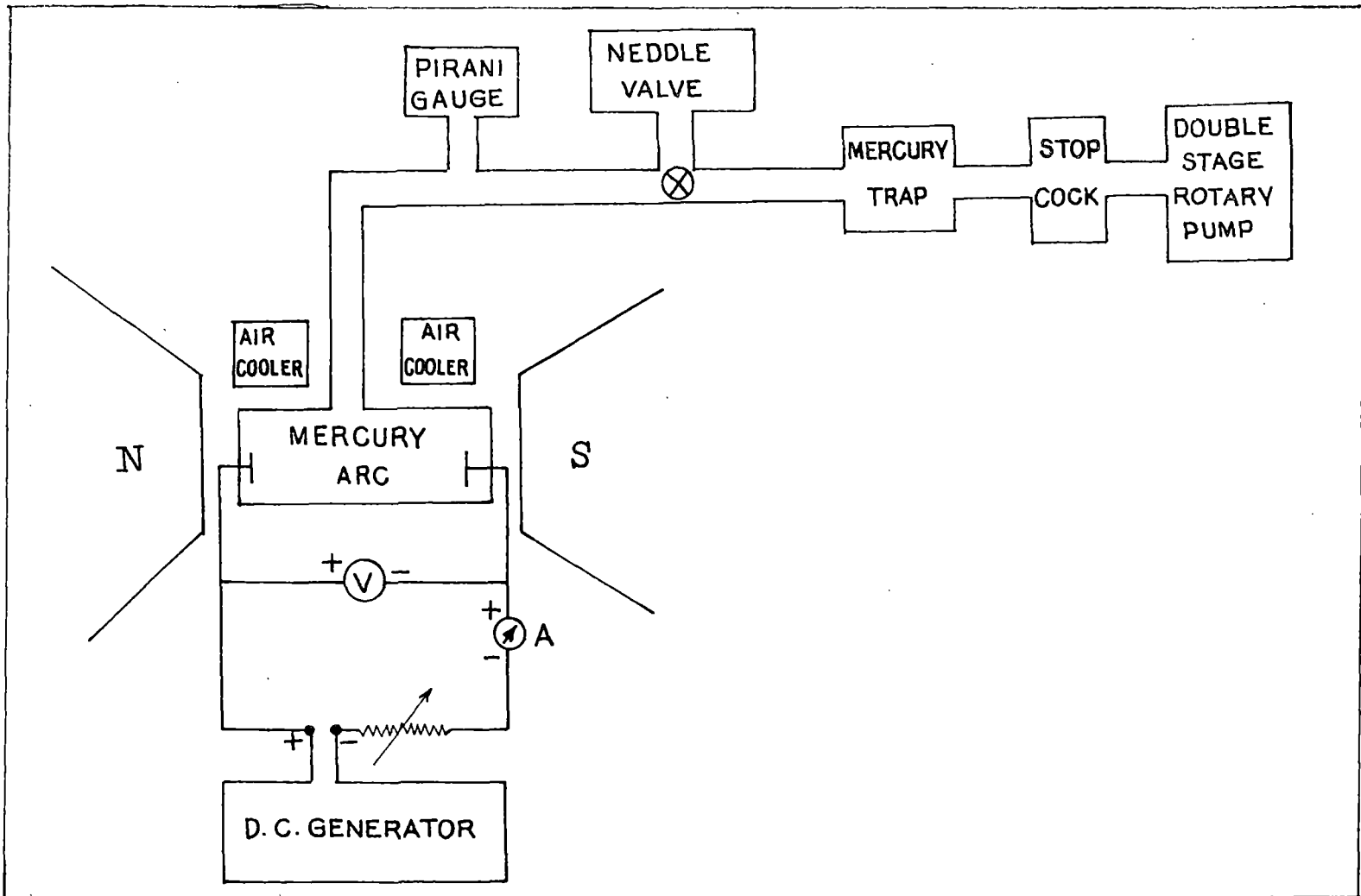


Fig. 2.4. Schematic diagram of experimental set-up in an axial magnetic field.

the arc tube, where investigations have been made, has been inserted between the pole pieces (fig. 2.5).

The magnetic field strength has been measured by gauss meter (Model G14). The electromagnets have been run by a stabilized dc power supply (Type EM20).

Both the mercury arc in the tube and some other metal arcs (in air) using Ag-Ag, Cu-Cu and Fe-Fe electrodes have been produced by a dc generator whose voltage may be adjusted by a rotary variable resistor fitted externally (in the front panel of a steel stand) and current can be adjusted with a rheostat inserted in series with the electrodes. The arc current has been varied upto 6-7 A. For photomultiplier tube, oscillator and dc amplifier the power supplies have been fabricated in the laboratory. The circuits for their fabrication have been taken from Radio Amateur's Hand Book (1965).

The calibration curves for the magnetic field for different set-ups have been shown in fig. 2.6, 2.7 and 2.8.

2.7. Determination of electron density  $n_e$  and electron temperature  $T_e$  in a mercury arc utilizing tungsten probe:

A cylindrical tungsten probe of 0.014 cm. radius within a glass capsule with a bare tip of 0.1 cm. height has been placed into the plasma at a separation of

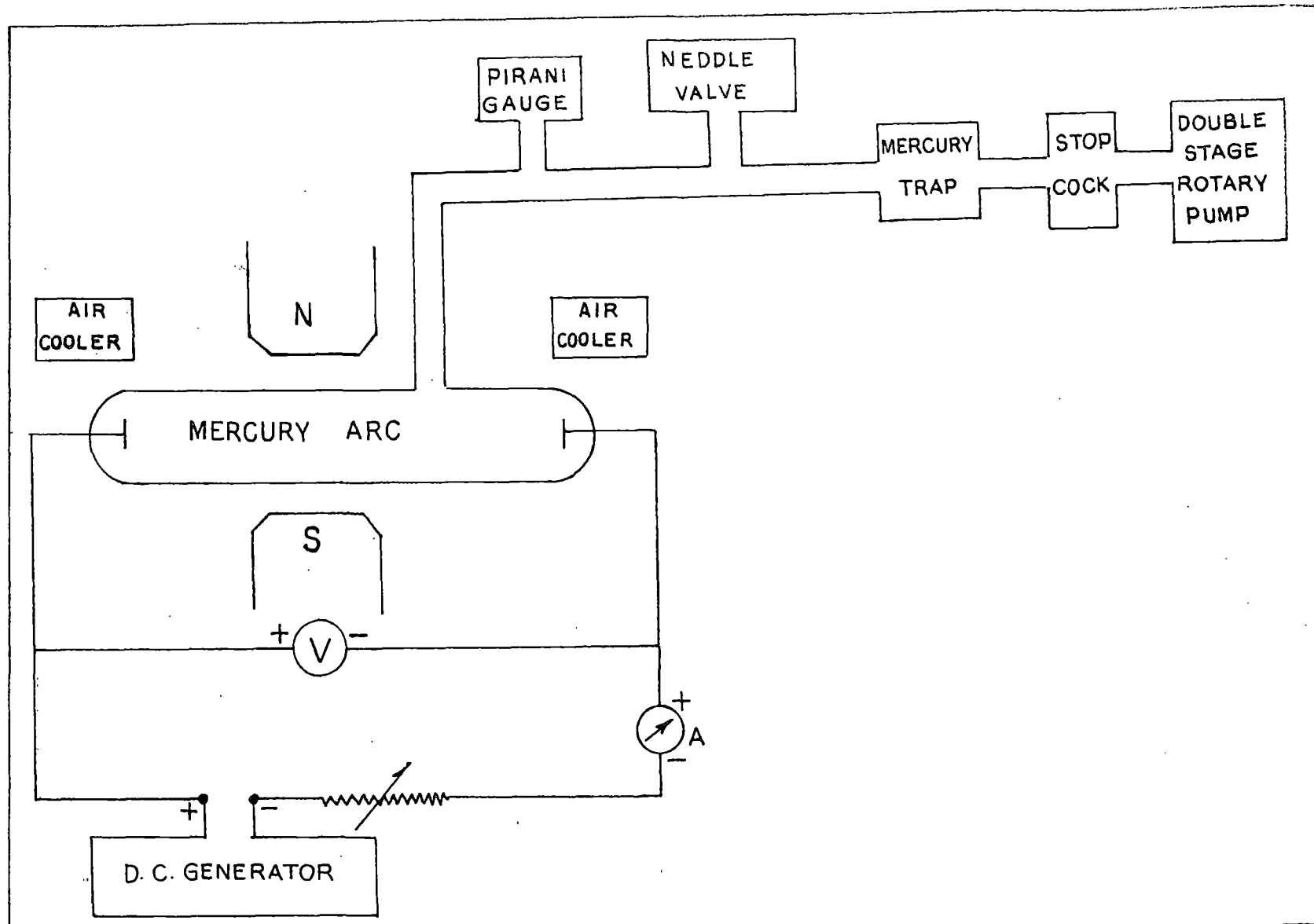


Fig. 2.5. Schematic diagram of experimental set-up in a transverse magnetic field.

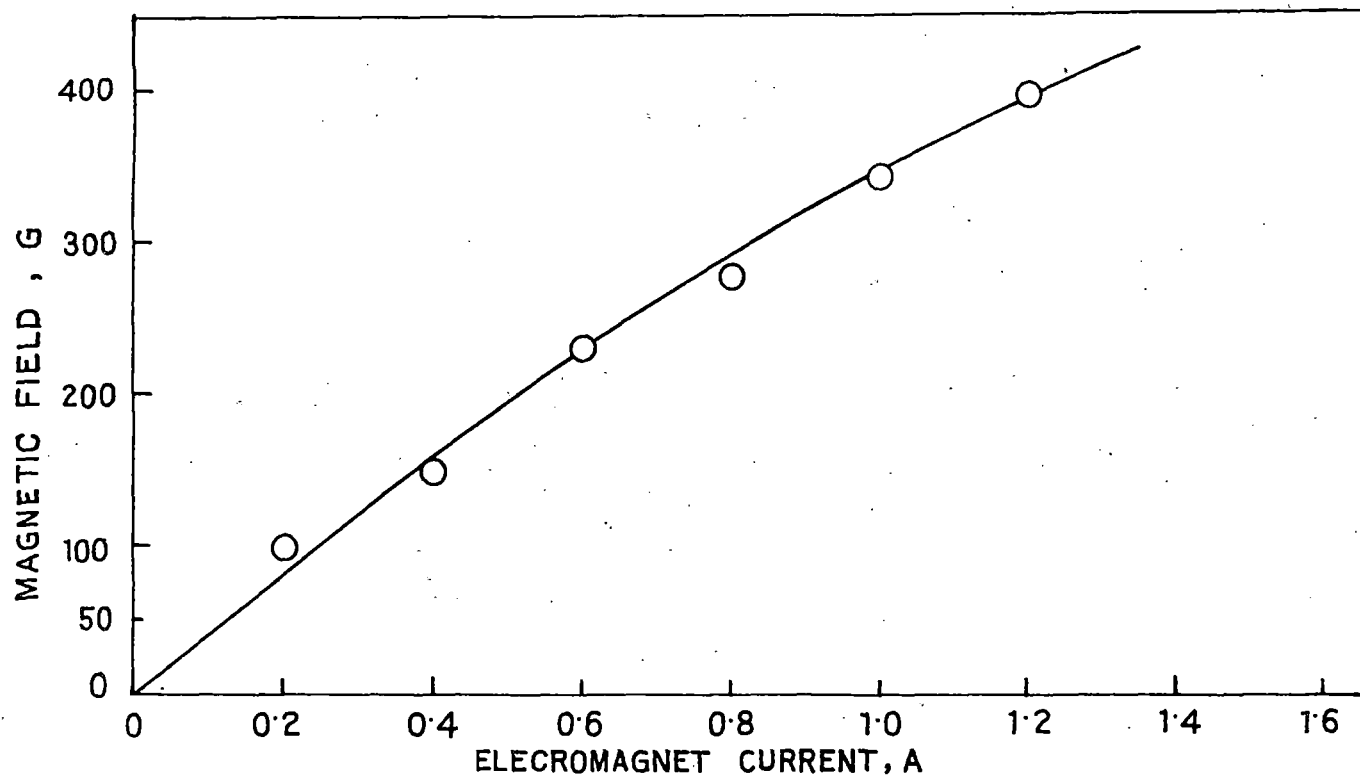


FIG. 2.6. MAGNETIC FIELD CALIBRATION CURVE, REF. CHAP. V.

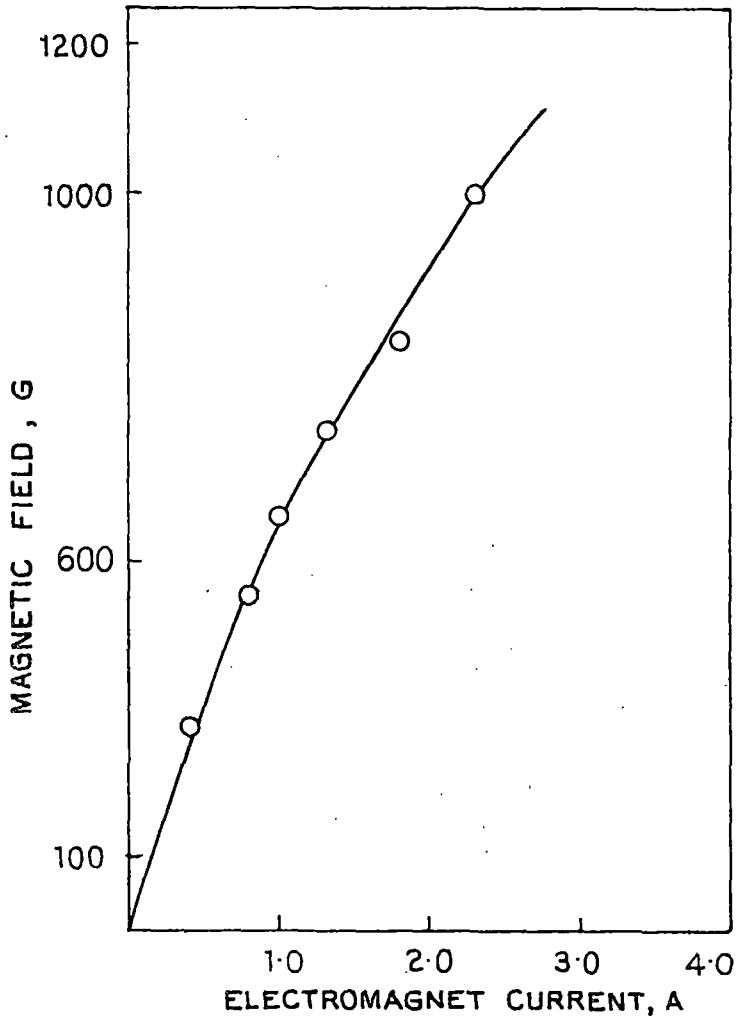


FIG. 2-7. MAGNETIC FIELD CALIBRATION CURVE  
REF. CHAP. VI.

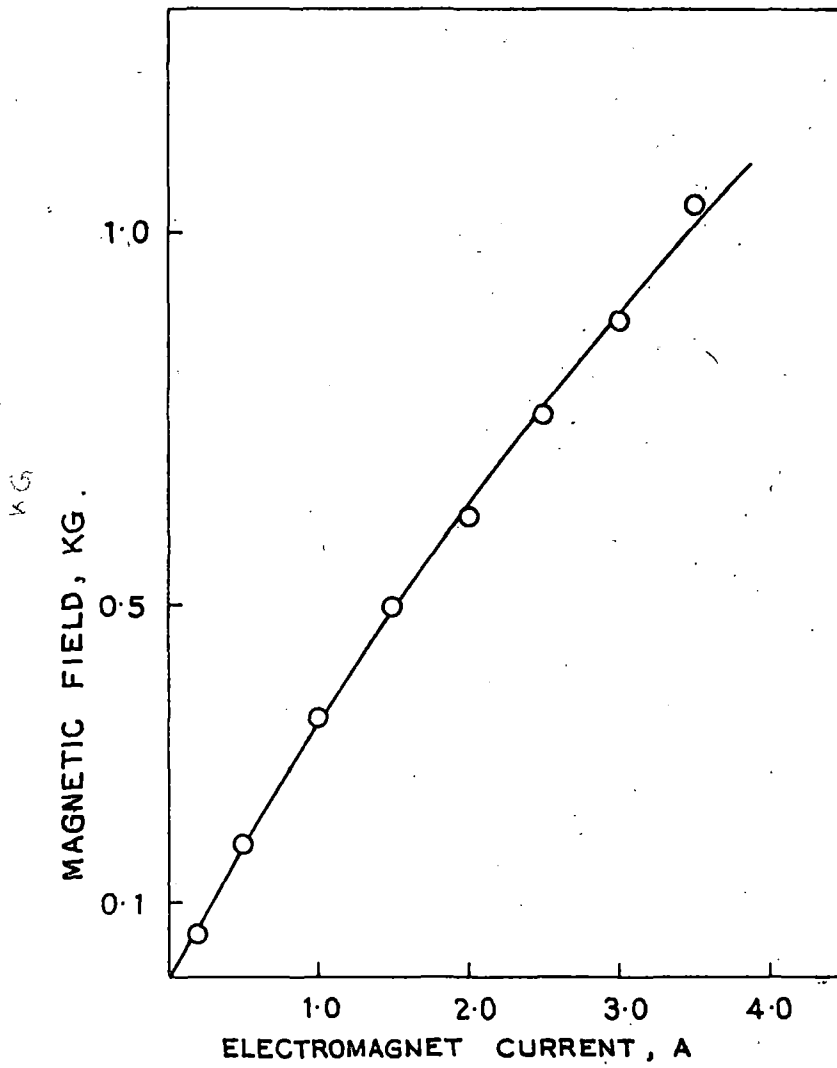


FIG. 2.8. MAGNETIC FIELD CALIBRATION CURVE, REF. CHAP. VI.

14 cm. from the anode of the tube as shown in fig.2.9(a) The tip of the probe is fixed accurately at the axis of the arc tube and the probe is perpendicular to the axis. In usual practice the height of probe ( $h$ ) should be larger than radius ( $r_p$ ) of the probe. But an upper limit of the ratio  $h/r_p$  may be calculated from the expression of electron saturation current to the probe

$$I_{e \langle \text{sat} \rangle} = -en_e A_p \left( \frac{T_e}{2\pi m} \right)^{1/2} \quad \dots(2.5)$$

where  $e$ ,  $n_e$ ,  $m$  and  $T_e$  are the charge, density, mass and temperature of electrons and  $A_p$  is the probe collecting area ( $A_p = 2\pi r_p h$ ). It is desirable that  $I_{e \langle \text{sat} \rangle}$  should not be large enough so that probe would not become too hot or incandescent and get damaged. In this investigation  $h/r_p$  is nearly 7.14. Both  $h$  and  $r_p$  have been measured by a travelling microscope. It will be discussed in chapter III that the results for the probe of these characteristic dimensions in arc plasma can be interpreted in the light of orbital theory.

The whole circuit arrangement for probe current measurement has already been shown in fig. 2.9(a). The probe is provided with dc potential from a series of dry batteries through a potentiometer.

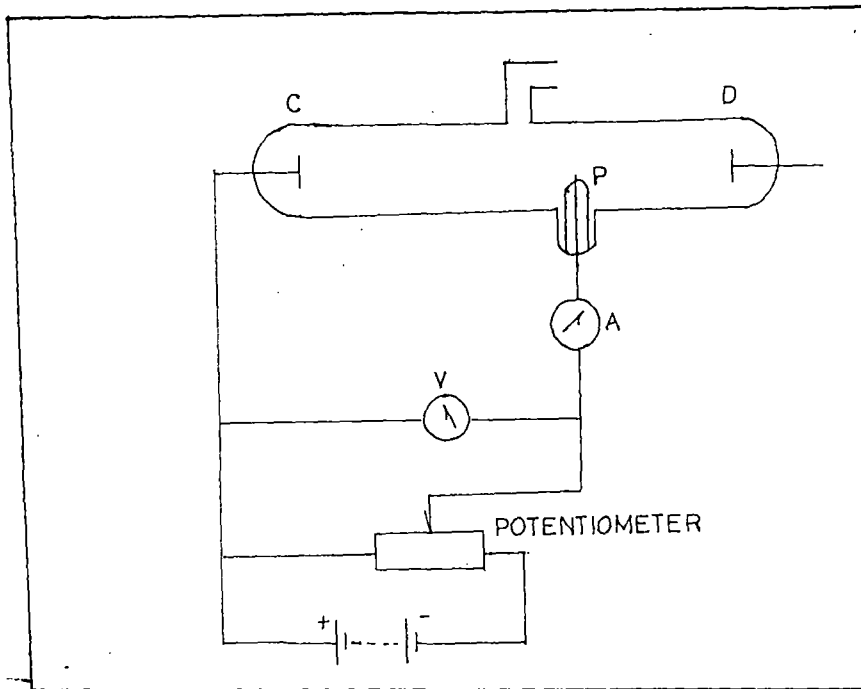


FIG. 2:9(a) SCHEMATIC EXPERIMENTAL ARRANGEMENT FOR MEASURING ELECTRON TEMPERATURE.

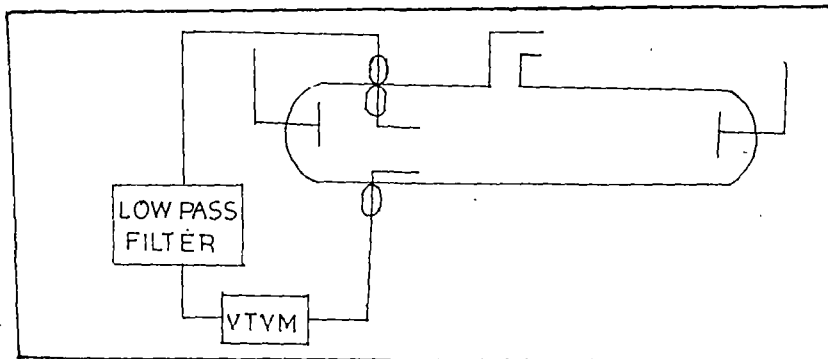


FIG. 2:9(b) SCHEMATIC EXPERIMENTAL ARRANGEMENT FOR MEASURING DIFFUSION VOLTAGE.

For changeover from ion current to electron current an external polarity reversal arrangement utilising manually operated band-switch is adopted to record the respective current. The probe circuit is connected to anode and the probe potential which is relatively negative with respect to anode has been varied in steps of 0.2 - 5 volts. The probe current which has been recorded, is the total current through the probe. Electron current  $I_e$  has been taken by subtracting ion current  $I_i$  from the total current

$$I_e = I_{tol} + |I_i| \quad \dots(2.6)$$

In our present experiment  $I_i$  is observed to be smaller than  $I_{tol}$  by a factor of order 1000. So effectively  $I_e$  equal to  $I_{tol}$ .

### 2.8. Diffusion voltage measurement by probes:

Two cylindrical tungsten probes of radius 0.014 cm. and height 0.8 cm. are inserted parallel to one another, one along the axis  $r = 0$  and the other at a separation of 0.6 cm. from the axis in the same cross sectional plane of the arc tube of 41 cm. length as shown in fig. 2.9 (b). The resultant voltage between the two probes has been recorded by a VTVM having an internal impedance of  $100 \text{ M}\Omega$ . A low pass filter circuit is provided at the output of the probes to

prevent oscillations generated in the arc from reaching the VTVM. The VTVM output gives the magnitude of the diffusion voltage. The diffusion voltage is recorded with variation of arc current from 2A to 5A for three background (buffer) air pressures (0.075 torr, 0.10 torr and 0.13 torr),

### 2.9. R.F. oscillator circuit:

The radiofrequency oscillator is of Hartley type; and the circuit diagram is shown in fig. 2.10(a). The range of frequency of this oscillator is from 3.3 MHz to 10.1 MHz. The inductance  $L$  of the tank circuit is divided into two parts  $L_1$  and  $L_2$  and their common point is connected to the cathode terminal of the vacuum tube 811. The end of  $L_1$  is connected to the grid through the parallel combination of  $R_g$  and  $C_g$ , which provides the grid bias potential. The end of  $L_2$  is connected to the plate of the oscillator valve 811 through the blocking capacitor  $C_c$ . Another variable gang condenser is inserted in parallel with the inductance (primary coil), thereby making a complete tank circuit. The current circulating in the resonant circuit passes through both parts of the inductance and develops a potential difference for the grid excitation. The direct component of the plate current is supplied from a stabilised high voltage power supply through a radio frequency choke.

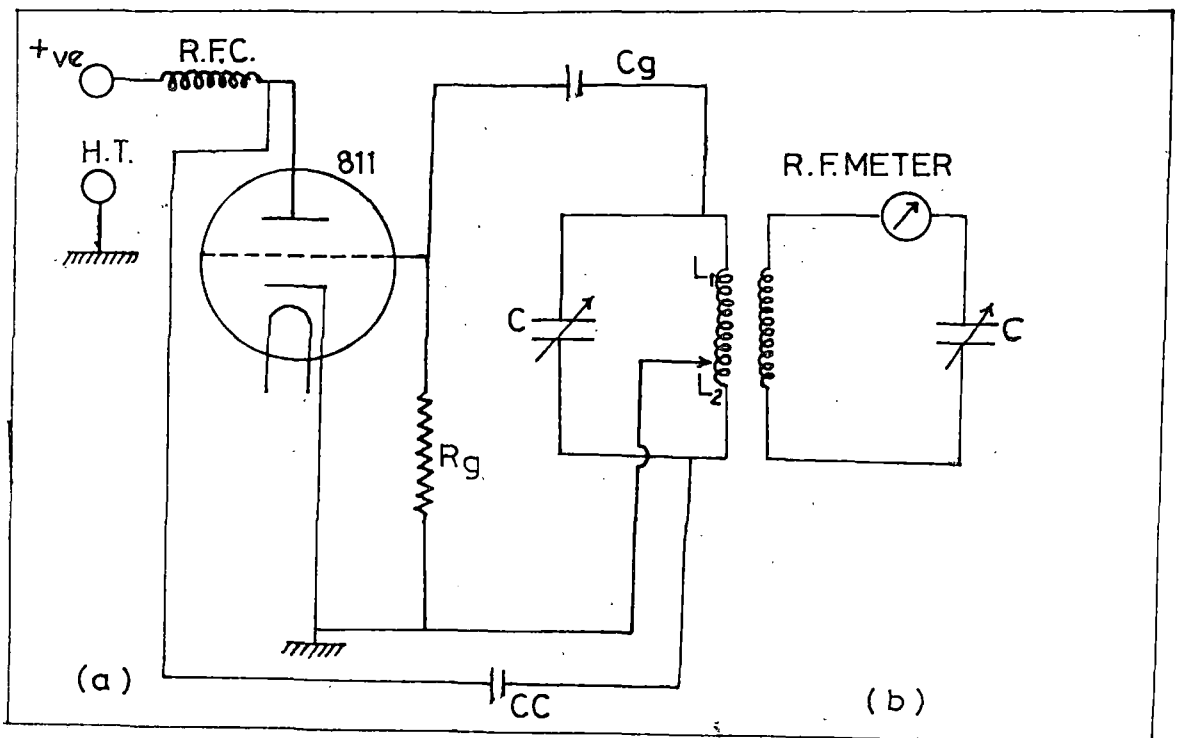


FIG.2:10. RADIO FREQUENCY OSCILLATOR CIRCUIT-(a); SECONDARY TUNING CIRCUIT -(b).

The blocking capacitor  $C_c$ , which has a small reactance compared with the load impedance, gives a path to the ac component, while the dc from the power supply is prevented. For a fixed gang condenser position, the oscillator frequency (3.69 MHz) has been measured in the experiment by an absorption wavemeter. The secondary receiving circuit consists of the coil wound around the arc tube, a variable tuning condenser and a radio frequency milliammeter (all connected in series, Fig. 2.10 (b)).

2.10. Measurement of electron atom collision frequency in an arc plasma by radiofrequency coil probe in conjunction with a longitudinal magnetic field:

In this diagnostic investigation a radio frequency coil probe technique has been employed to find electron - atom collision frequency in an arc plasma in presence of axial magnetic field. An arc tube made of pyrex glass of length 10.8 cms. and diameter 1.83 cm. is used. Besides the two tungsten mercury pool electrodes at the two ends, other two tungsten probes have been introduced upto the axis of the tube in the positive column with a separation of 4.6 cm.

as shown in fig. 2.11. A small coil of length 4.5 cm has been wrapped around the tube in the region of probe to probe separation. These coils supply radio frequency power induction from the externally applied high frequency oscillator. The arc tube was placed inside the two pole pieces of an electromagnet separated by 11.5 cm.

A radiofrequency milliammeter ranging from 0 to 120 mA (Thermocouple type) made by Weston Instruments, Inc. (USA Model No. 308) in series with a variable gang condenser has been connected at the two ends of the coil wound around the arc tube. These three elements connected in series act as a secondary tank circuit in the investigation.

The oscillator coil is placed near the work coil i.e. the coil wound surrounding the arc tube, and the induced rf potential is tuned with the variable condenser inserted in the secondary circuit in series with the rf milliammeter and the work coil. The arc is then produced by adopting the tilting process. Subsequently the rf meter indicator shifts from its previous position. The tuning condition is achieved by the variable gang condenser. A number of aircoolers and a water circulation system have been provided for controlling the arc temperature and to maintain a steady wall temperature. The rf meter reading is then recorded as far accurately

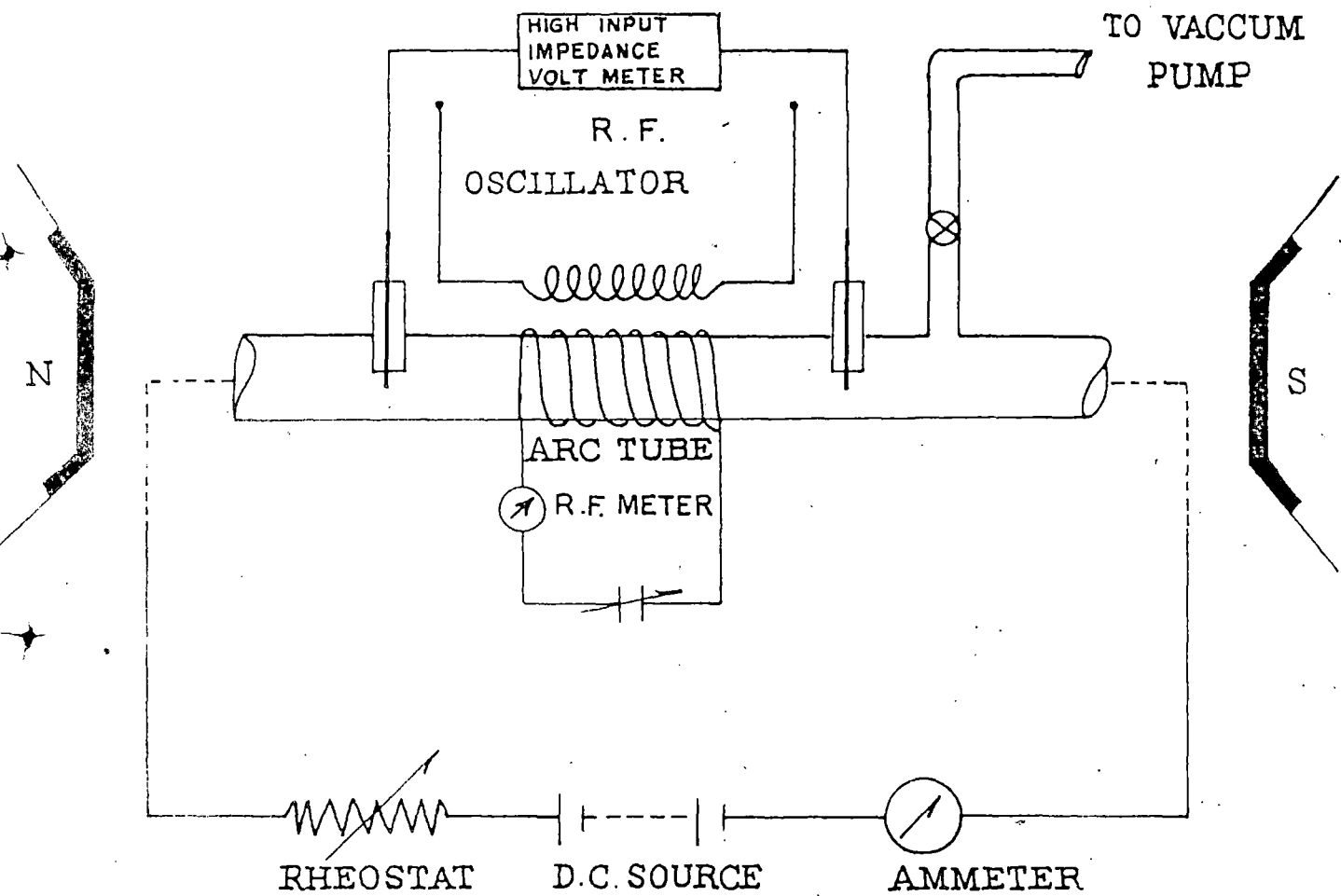


Fig.2.11. Schematic Experimental Arrangement for the study of Arc Plasma characteristics in Presence of Longitudinal Magnetic field .

as possible. This current reading is  $i_1$ . Then the voltage across the two probes inserted in the positive column has been measured by an electronic multimeter with high input impedance. Now without disturbing any arrangement of the circuit the arc is switched off. The meter recording pointer again shifts from its previous position. The tuning condition is again set by the condenser and the tuned current  $i_0$  is recorded.

Before starting the experiment the magnetic field was first calibrated with current (Fig. 2.6).

The sequence of observations and measurements are given in the following paragraph :

The arc tube was placed in between the two pole pieces of electromagnet so that it may be tilted freely to strike it. The tube was placed along the magnetic field so that any radial magnetic field component should vanish. To maintain the desired discharge current rheostats were adjusted. The probe coil was tuned and the rf current  $i$  ( i.e. the coil probe current in arc on condition and in absence of magnetic field) was noted. In this condition the probe to probe voltage  $E$  was noted. When the magnetic field was applied, the probe to probe voltage and discharge current decreased. In presence of the axial magnetic field

the coil probe current  $i_B$  was noted. To avoid extinction of the arc for lower discharge current, the discharge current  $I_B$  was adjusted to its previous value  $I$  in presence of magnetic field and again  $E_B$  and  $I_B$  were noted simultaneously. Now both the magnet and the arc were turned off. The coil probe was returned and the tuned current  $i_0$  i.e. the coil probe current in absence of plasma was noted. The whole procedure was repeated a number of times. The observation has been carried out for a fixed oscillator frequency 3.69 MHz.

The variation of the quantity  $(\alpha - 1)$  where  $\alpha = i_0/i_1$  is proportional to the arc current 'I'. In this experiment each time the arc current was changed, sufficient time was allowed to pass to ensure equilibrium before any measurement [ $E$  or  $(\alpha - 1)$ ] was made.  $(\alpha - 1)$  and  $E$  varied linearly with the arc current. But due to application of axial magnetic field the value of  $E$  and  $(\alpha - 1)$  decreased slowly with the increasing magnetic field. It was found that if the arc currents were in the low side, the reduction of current due to the application of axial magnetic field some times caused extinction of the arc. To remove this difficulty, immediately after applying the magnetic field the arc current was adjusted to its original

value when necessary. But it has been shown that the collision frequency was constant for various magnetic field at particular arc current.

2.11. Evaluation of electron temperature in transverse and axial magnetic field in an arc plasma by measurement of diffusion voltage:

For measurement of diffusion voltage in presence of transverse magnetic field the arc tube of 41 cm. length, 26.5 cm. anode-cathode spacing, 2.2 cm. inner diameter and 2.5 cm. outer diameter has been utilised and in presence of longitudinal magnetic field the arc tube is of 9.1 cm. length, 6.2 cm. anode - cathode spacing, 1.86 cm. inner diameter and 2.16 cm. outer diameter. The arc is energised by a dc generator with a rheostat to change the current through the arc. The whole arc is cooled by air coolers and two mercury pool electrodes by water circulation. To maintain the background pressure fixed in the arc vessel, dehydrated air is introduced with an arrangement of needle valve which is suitably filled in the vacuum arrangement. For determination of plasma parameters in transverse magnetic field the positive column of the mercury arc is kept between the pole pieces of electromagnet while for that measurement in axial magnetic field the whole arc tube has been placed between the pole pieces.

As in previous articles, similarly two cylindrical tungsten wires of 0.014 cm. and 0.8 cm. height have been set parallel to one another one along the axis  $r = 0$  and the other at a separation of 0.6 cm. from the axis in the same cross sectional plane of the tube. But these two probes in case of axial magnetic field are of 0.53 cm. height while other specifications remain same as in transverse magnetic field.

In both magnetic fields the output voltage at the two probes has been measured by a VTVM. It is actually the low pass filter output, as a low pass filter is connected at the output of the probes to prevent noise caused by oscillation in the arc from reaching in the VTVM. The diffusion voltage has been recorded as a function of the magnetic field with arc current as a parameter. For transverse magnetic field the diffusion voltage has been recorded upto the magnetic field 1000 G at three fixed arc currents namely 2.5 A, 3.0 A, and 3.5 A, and in axial magnetic field upto 1010 gauss at three fixed arc currents namely 3.0 A, 4.0 A and 5.0 A.

## 2.12. Diagonostics by spectroscopic method:

To estimate the plasma parameters spectroscopic method has been utilized. Fig. 2.12 and Fig. 2.13 show a detailed schematic diagram of this experimental set up. The radiations from the axial regions of vertical discharge tube passing through a vertical slit is focussed by a double convex lens on the vertical slit of the collimator of the spectrograph. There is a Pellin-Broca prism for 90 degree deflection of the spectrum in the spectrograph. Such a mounting is essential as a monochromator is mounted with the fixed slit. The exit slit is perpendicular to the plasma source. The wavelength (arc and glow spectral lines) of the source is changed by rotating the prism with a mechanical arrangement fitted with an accurately calibrated drum. From Handbook of Chemistry and Physics Hodgman (1956), the wavelengths of the visible spectrum have been checked.

In general, this type of apparatus has a low resolving power which would be advantageous in the present investigations, because it is unable to resolve Zeeman splitting. The slit width ranging from 0.25 mm to 1 mm. can be varied with a micrometer arrangement, depending on the response of lines chosen to the photomultiplier. The slit width has been kept constant for a set of observation.

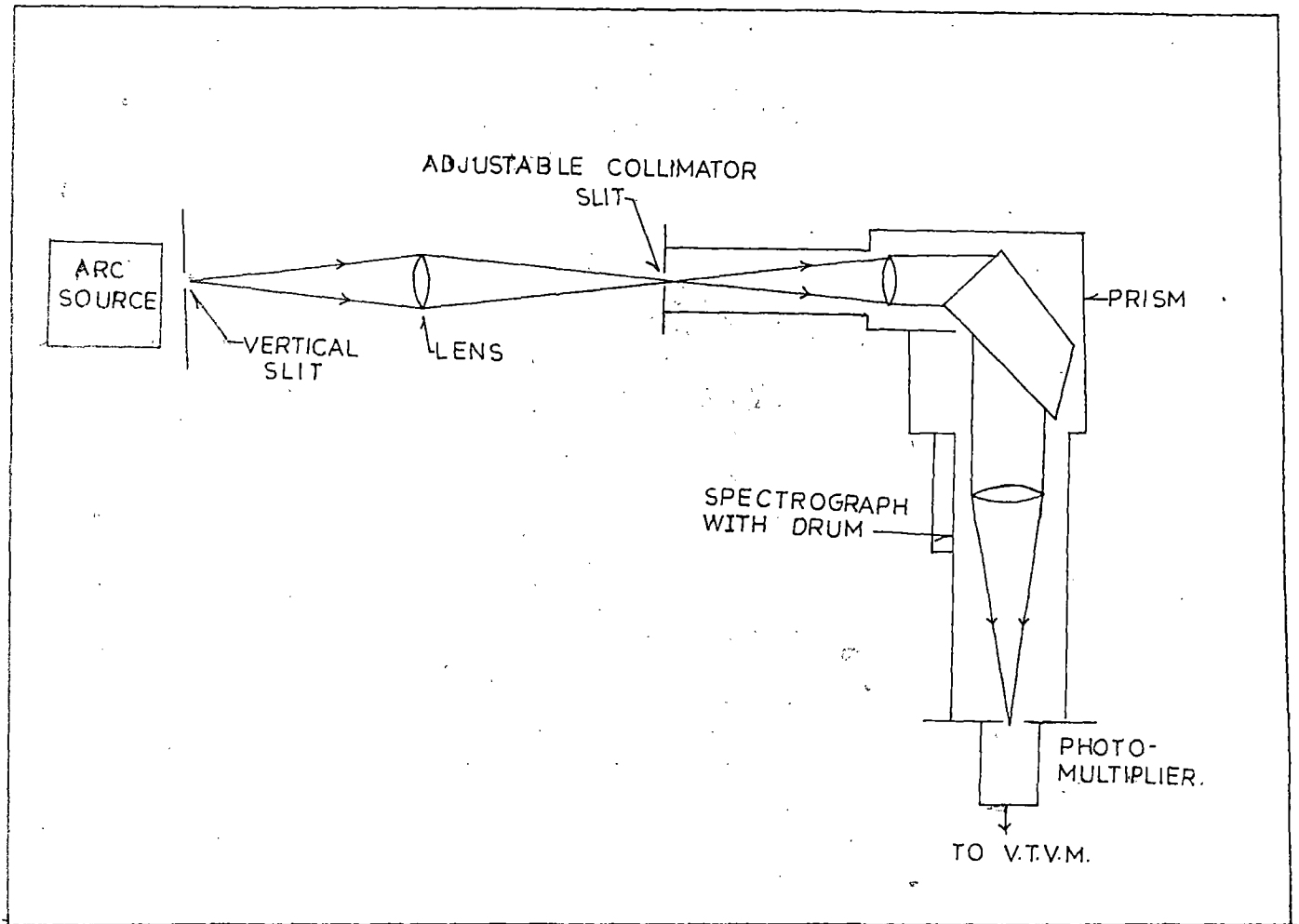


Fig. 2-12. Experimental set up for spectroscopic measurements.

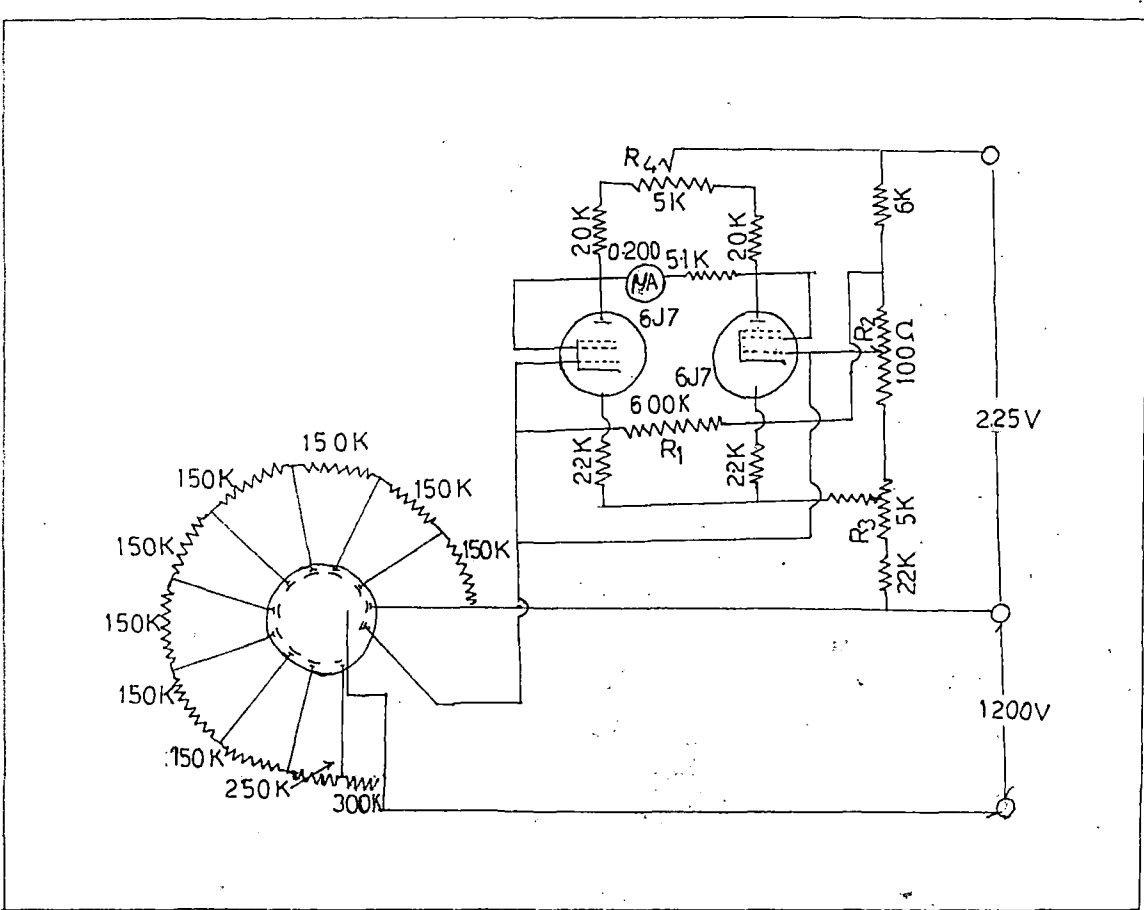


FIG. 2.13

PHOTOMULTIPLIER CIRCUIT.

For measuring  $T_e$ , two criteria for suitable line choice may be mentioned:-

(1) The energy of separation of the upper states of the two transitions chosen should be comparable to the value of  $T_e$ . But this is not possible always. In the visible region for two lines which have sufficient response to the detector the energy of separation of upper states becomes sometimes smaller than the value of  $T_e$ . One of the remedy that is suggested is to use one of the ionic lines and one atomic line.

(2) The lines should be such that in the near vicinity there would be no other line, so that

$\int_0^\infty I_\nu d\nu$  is the measure of total intensity of a radiation with frequency  $\nu$  and in our investigation slit widths are comparatively wide enough as to detect the total intensity of radiation.

The selected spectral line has been focussed on the cathode of the photomultiplier tube MI OFS29V $\lambda$  operated at 1425 V, whereas the collimator is focussed by rock and pinion arrangements. Behind the eyepiece of the spectrograph the top cathode type photomultiplier which has low mean radiation equivalence of dark current is placed in a darkened ebonite housing. The power source of photomultiplier is provided in two sections : the first is 1200 v stabilized to supply

the dynode voltage and the second is to provide 225 V between the final dynode and the anode as in Fig.2.13. To operate the VTVM the second voltage source is used. It consists of two 6J7 tubes operated at 32V on the plates and 1.3 V negative grid bias. The grids are connected to the two ends of a resistor R (600 K $\Omega$ ) which is in series with the plate of the photomultiplier. A potential drop developed, when current flows through the resistor  $R_1$  and one of the 6J7 tubes draws less current producing an imbalance in the plate circuit. A 0-200  $\mu$  A meter is connected in between the plates of the 6J7 tubes to measure this unbalanced current. For this circuit arrangement for a signal 3V, the 6J7 tubes reached cut-off and beyond which there is no further increase in the meter deflection.

The microammeter is set to zero with  $R_2$  and a coarse balance is made with  $R_4$  with no radiation on the photomultiplier tube. In this way the effect of dark current in actual measurement of radiation is completely minimised. With 3V or a little more applied to resistor  $R_1$ , the meter is set to full scale deflection with the help of another resistor  $R_3$ . The radiation of the spectral line under investigation is recorded at the output by microammeter. The slit of the

spectrograph is varied in such a way that meter deflection corresponding to the spectral line with strongest response to the photomultiplier is in the full scale range of the meter.

The sensitivity of a photomultiplier depends on wavelength of incident radiation and on quantum efficiency of the cathode material (including the effect of photomultiplier's window material). A characteristic of quantum efficiency of MIOFS29V<sub>λ</sub> against wavelengths is plotted taking the values from Carl Zeiss brochure no. 40 - 637 - 2, in Fig.2.14. From this plot the cathode radiant sensitivity S in amperes per watt corresponding to a radiation of wavelength λ (Å) is calculated as

$$S = \frac{Q \lambda}{12395 \times 100} \quad \dots(2.7)$$

here Q is the percentage quantum efficiency. The relative spectral sensitivity for two lines are calculated and the microammeter reading for total intensities of lines are corrected for relative spectral response of the photomultiplier from the determined value of S. The emissive frequency  $\nu$  is directly proportional to observed total intensity which can be separated into a continuous and discrete

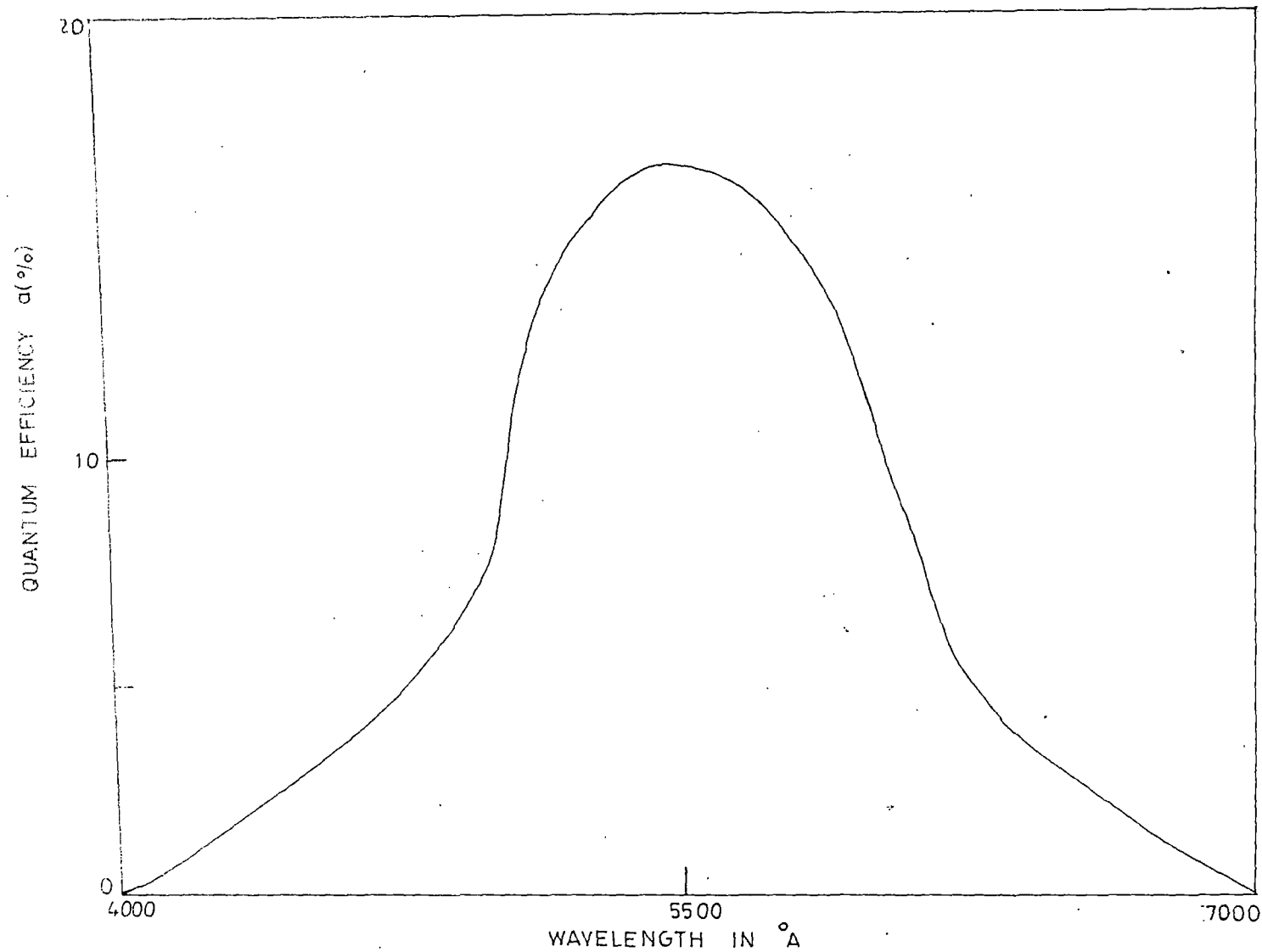


FIG. 2.14. QUANTUM EFFICIENCY IN % OF PHOTOMULTIPLIER M10F 529V<sub>λ</sub>  
(VEB CARL ZEISS JENA BROCHURE NO. 40-637-2.)

part

$$\epsilon_{\lambda} = \epsilon_{\lambda,C} + \epsilon_{\lambda,L} \quad \dots(2.8)$$

$\epsilon_{\lambda,L}$  contains the  $\lambda$  desired spontaneously emitted energy within the line,  $\epsilon_{\lambda,C}$  is eliminated by balancing the VTVM to the null of meter reading with resistors in the circuit when the continuum radiation at the near vicinity at the line is focussed on the photomultiplier tube cathode and the contribution for  $\epsilon_{\lambda,C}$  is to be negligibly small.

2.13. Measurement of intensity enhancement of spectral lines with increasing arc current in arc plasma:

Two respective metal electrodes of a particular arc have been fixed with a vertical stand as shown in fig. 2.15, where upper metal electrode is attached to a vertically movable bench arrangement with the help of a screw. Initially the two electrodes are brought into contact by this screw. A dc source with an adjustable rheostat and an ammeter, is utilized to produce the arc namely for Ag-Ag, Cu-Cu and Fe-Fe in air. An accurately calibrated constant

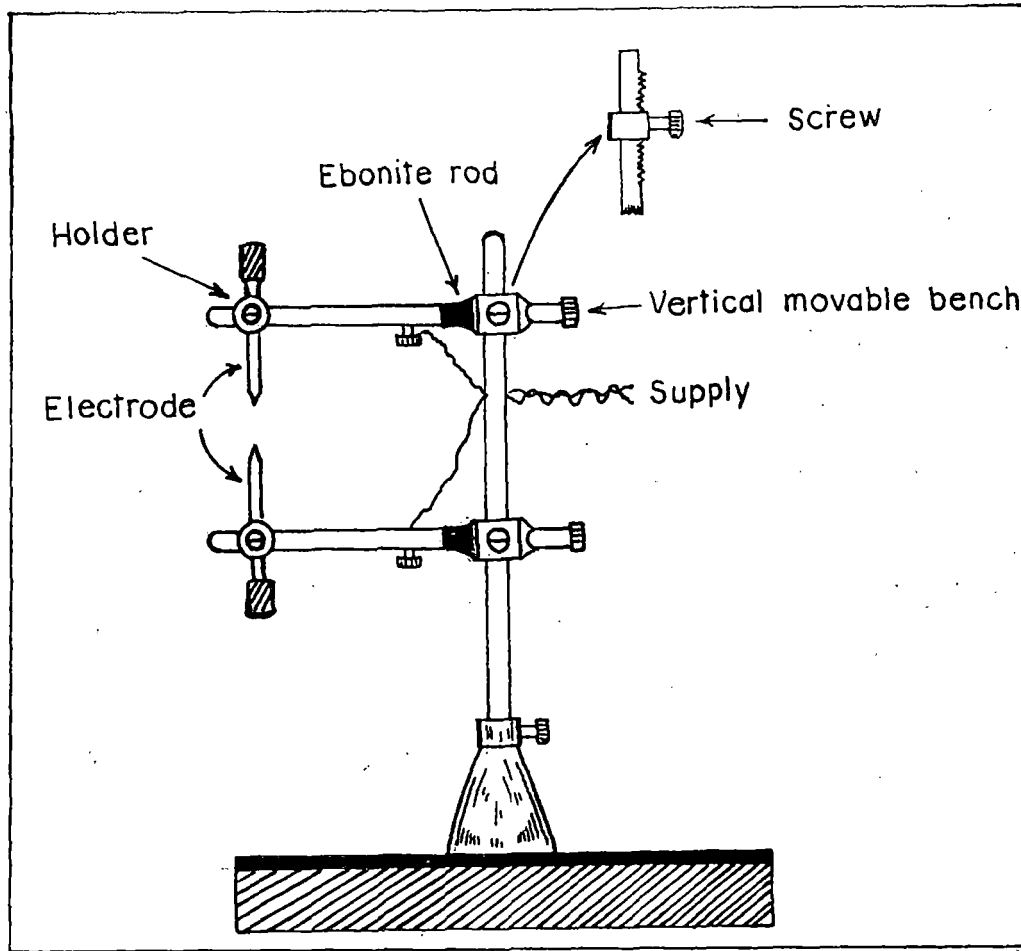


FIG. 2-15. METAL ARC ARRANGEMENT

deviation spectrograph has been used to measure the wavelength of the spectral lines of the arc sources. Each line is focussed on the cathode of the photomultiplier tube M10 FS29V<sub>λ</sub>, and intensities are thus obtained by measuring the output of the photomultiplier which is measured by a difference amplifier. The whole arrangement of this spectroscopic part - its arrangement and its electronics circuit is given in the previous section.

The output microammeter current recorded in the difference amplifier is observed to be linearly proportional to the known spectral line intensities and the slit width of the spectrograph has been adjusted to obtain a large deflection in the microammeter, thereby enhancing the desired level of sensitivity in the measurement of the line intensity ratio. In case of silver electrodes the arc current is varied from 3A to 7A and in case of copper and iron electrode the variation is 2.5 A to 5 A.

2.14. Spectroscopic investigation in air and hydrogen discharges heated by repeated discharge of a bank of condensers:

A spectroscopic method is to be operated for measurements of electron temperature and electron density to which plasma can be raised by utilizing the bank condenser discharge. In this experimental

arrangement a discharge tube of length 8 cm. having four electrodes is used. Electrodes are circular and parallel to each other. The discharge tube is connected to exhaust pump through glass tubes. Air and prepared hydrogen have been passed through dilute solution of caustic potash to remove traces of  $\text{CO}_2$  and is then washed with water by passing through series of wash bottles containing cold water to remove traces of caustic potash, dust particles and organic matters. It has been dried by passing through a tower of fused  $\text{CaCl}_2$  and finally through  $\text{P}_2\text{O}_5$ . The pressure inside the discharge tube has been kept constant by means of a needle valve and by utilizing Mcleod gauge pressure is measured. The separation between two electrodes is 2.95 cm. to which voltage (50 cycle ac) through variac is applied for breakdown of gases. By two electrodes separated by a distance 0.85 cm. a discharge from eight charged condensers (each of 24  $\mu\text{F}$ ) connected in parallel, has been passed. The whole spectroscopic method has been discussed in article 2.12. By utilizing this method, the enhancement of current before and after bank condenser discharge has been noted by a microammeter for a particular spectral line and hence repeated for the other lines. The enhancement of discharge current is also noted by milliammeter

between two electrodes through which condenser discharge has been passed. The above procedure is repeated for 2250 volts, 2000 volts, 1750 volts and 1500 volts discharge voltages for 0.2 torr pressure in case of air glow and for 0.7 torr pressure in case of hydrogen glow. The whole experimental arrangement is as shown in Fig. 2.16.

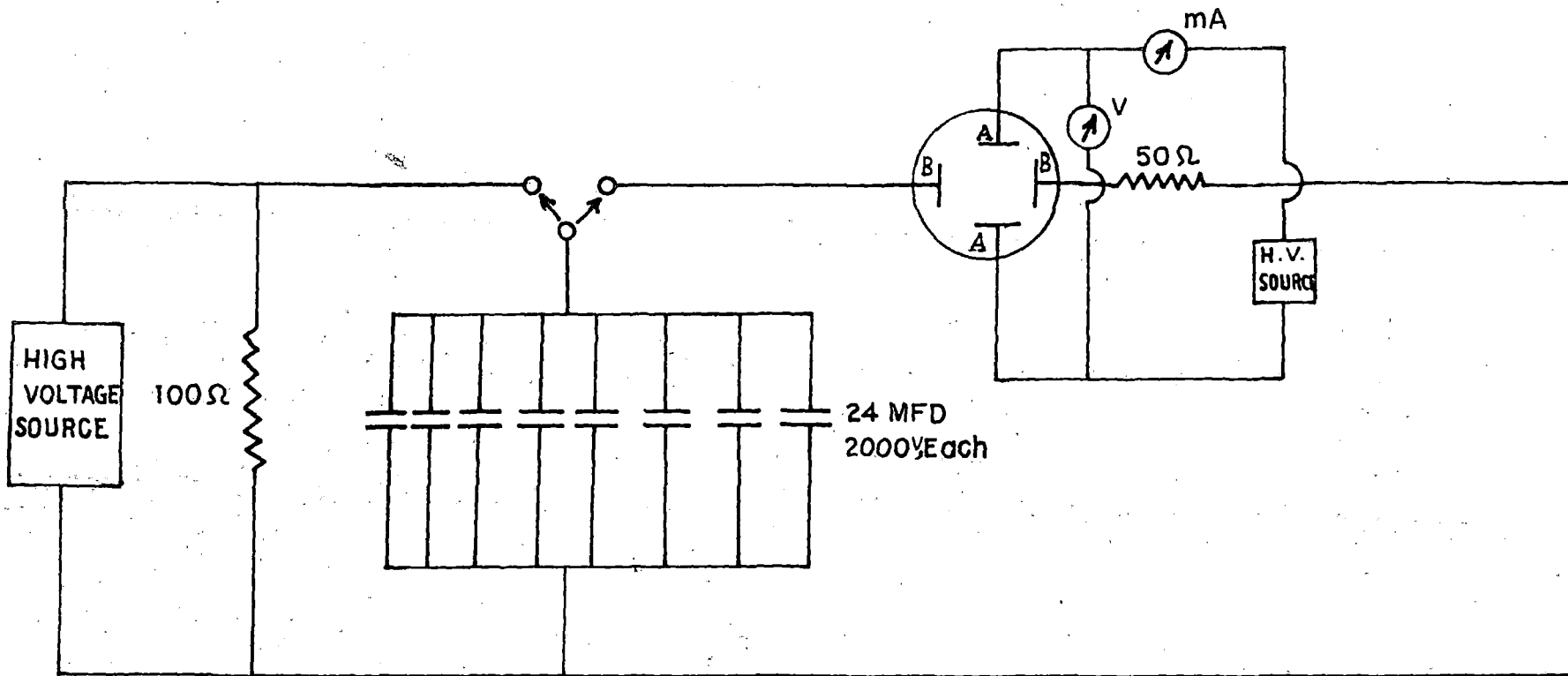


FIG. 2-16. ENHANCEMENT OF SPECTRAL INTENSITY BY BANK CONDENSER DISCHARGE .

References:

1. Dushman, S. and Lafferty, J.M. (1962)  
Scientific Foundations of Vacuum Techniques,  
2nd. Edn. (John Wiley, New York).
2. Hodgman, C.D. (1956), Handbook of Chemistry  
and Physics, 38th. Edn. (Chemical Rubber  
Publishing Co., Ohio).
3. Lamar, E.S. and Compton, K.T. (1931), Phys.  
Rev. 37, 1069.
4. Radio Amature's Hand Book (1965), 42nd. Edn.  
American radio relay league, West Hartford)
5. Verweij, W. (1960), Philips Res. Rep.  
Suppl. No. 2